

## ESTIMATION OF CROWN CLOSURE FROM AVIRIS DATA USING REGRESSION ANALYSIS

K. Staenz<sup>1</sup>, D.J. Williams<sup>2</sup>, M. Truchon<sup>1</sup>, and R. Fritz<sup>3</sup>

<sup>1</sup>Canada Centre for Remote Sensing  
588 Booth Street, Ottawa, Ontario, Canada K1A 0Y7

<sup>2</sup>MacDonald Dettwiler and Associates Ltd.  
13800 Commerce Parkway, Richmond, British Columbia, Canada V6V 2J3

<sup>3</sup>University of Freiburg  
Werderring 4, 7800 Freiburg, Germany

### 1. INTRODUCTION

Crown closure is one of the input parameters used for forest growth and yield modelling. Preliminary work by Staenz et al. (1991) indicates that imaging spectrometer data acquired with sensors such as the Airborne Visible/Infrared Imaging Spectrometer (AVIRIS) have some potential for estimating crown closure on a stand level. The objectives of this paper are (a) to establish a relationship between AVIRIS data and the crown closure derived from aerial photography of a forested test site within the Interior Douglas Fir biogeoclimatic zone in British Columbia, Canada, (b) to investigate the impact of atmospheric effects and the forest background on the correlation between AVIRIS data and crown closure estimates, and (c) to improve this relationship using multiple regression analysis.

### 2. DATA ACQUISITION

AVIRIS data of the test scene used for this investigation were collected in British Columbia, Canada, on August 14, 1990. Additional information includes aerial photography of 1:25000 scale and British Columbia Ministry of Forests's Geographic Information System (GIS) on a 1:20,000 scale encompassing forest inventory maps and forest attribute information. This flat area mainly covered by douglas fir (*Pseudotsuga menziesii* var. *latifolia* (Mirb.) Franco) with inclusion of lodgepole pine (*Pinus contorta* Dougl.) and yellow pine (*Pinus ponderosa* Laws.) is situated between the Columbia and Kootenay Rivers. The 30 to 200 year old forest stands were selectively logged several times over the years resulting in a full range of crown closures. The open forested areas are mainly covered by dry grass while the background material for stands with high crown closure consists of a mixture of soil and litter.

### 3. ANALYSIS SCHEME

Radiometrically calibrated AVIRIS data were corrected for atmospheric effects using in a first step an altitude dependent version of the 5S code (Teillet and Santer, 1991) for a viewing angle dependent removal of the scattering effects and, secondly, the flat field approach for a first order correction of the gaseous transmittance. The combination of these procedures for the removal of atmospheric effects was first successfully demonstrated by Staenz et al. (1991) and is shown in Figure 1 for spectra of different crown closure classes. A total of 159 bands (508.40 - 2357.80 nm) were processed for subsequent analysis after eliminating the strong water vapour absorption bands around 1400 nm and 1900 nm as well as the first few bands predominated by noise patterns and the last ones due to a low signal-to-noise ratio (SNR). Overlapping bands between the spectrometers were also eliminated keeping the bands of the spectrometer with the higher SNR.

Homogeneous forest stands with different crown closures were initially

selected from the forest cover maps using in addition the GIS attribute information characterizing each forest stand (polygon). For this purpose, the forest cover maps were registered to the AVIRIS scene with the nearest neighbour resampling technique resulting in an RMS error of  $\pm 1.50$  pixels in the pixel direction and  $\pm 0.95$  pixels in the line direction. The percent crown closures of these stands were then checked with black and white aerial photography on 1:25,000 scale and re-adjusted where necessary. Additional samples were selected from the aerial photography and transferred to the AVIRIS scenes to cover the full range of percent crown closure. Spectra as shown in Figure 1 were then extracted for each of the 26 sample sites encompassing between 27 and 199 pixels, and grouped into 10 crown closure classes (0, 10, 20, 30, 40, 50, 70, 80, 90, and 100 percent).

Linear regression analysis was first applied to the radiance and relative reflectance data (atmospherically corrected) to determine their relationship with crown closure at each band. In addition, spectral derivatives (first-order, second order) to reduce the background noise were calculated from atmospherically corrected data and included in the regression analysis as well. In a second attempt, an exhaustive stepwise multiple regression procedure STEPWISE from S-PLUS (1991) was used to find band combinations with significantly higher correlation than with the univariate analysis.

#### 4. RESULTS

Coefficients of determination ( $R^2$ ) calculated at each spectral band are shown in Figure 2 for the radiance and the relative reflectance (atmospherically corrected) data, as well as the first-order derivative of the relative reflectance spectra. The  $R^2$  values exceed 0.8 in many of the non-derivative spectral bands as shown, for instance, for band 204 (2258.3 nm) in Figure 3. It can also be seen from Figure 2 that the application of the atmospheric correction procedure significantly increased the  $R^2$  values in most of the bands within the 700 to 1350 nm region. The procedure produces in addition slightly higher  $R^2$  values between 500 nm and 580 nm and lower  $R^2$  values between 580 nm and 700 nm. The non-derivative-band  $R^2$  values generally outperform the derivative-band  $R^2$  values considerably except between 750 nm and 860 nm for the radiance data. The high spectral variability in the derivative-based  $R^2$  values is expected since derivatives are sensitive to high frequency noise and spectra with a similar shape produce similar values (zero-crossing points) at specific wavelengths along the derivative curves (Gong et al., 1992). These effects could reduce the correlation between derivative spectra and crown closure.

Stepwise multiple regression analyses of relative reflectance (159 bands) spectra were applied to the entire data set as well as to a reduced set of nine bands (Table 1). These bands were selected based on their known relationships with biomass, chlorophyll, liquid water content, cellulose, etc. It can be seen from Table 1 that the multivariate analysis improves the correlation between the AVIRIS data and crown closure for both data sets.  $R^2$  values larger than 0.9 can be achieved with this procedure as shown graphically in Figure 4 for the best five-band subset of the nine-band data. Furthermore, the prediction of crown closure improves using the entire data set in the analysis procedure. However, the  $R^2$  values should be interpreted with caution since an inflation of  $R^2$  occurs when the predictor variables (159 bands) outnumber the sample size (26) (Wessman et al., 1989). Significance tests at the 0.95 confidence interval for  $R^2$  values obtained with the stepwise multiple regression techniques were therefore based on adjusted values of  $R^2$  (Rechner and Pun, 1980).

The correlation achieved with the regression procedures could be affected by noise in the data caused by the sensor system and the atmospheric correction procedure. However, the robustness of the regression results with respect to noise is not known, but will be considered for future analysis.

## 5. CONCLUSION

Univariate as well as multivariate regression analyses were applied to an AVIRIS data set acquired over a forested test site in British Columbia, Canada to investigate the relationships between crown closure and the AVIRIS data. Values of  $R^2$  larger than 0.8 were achieved in many spectral bands for the atmospherically corrected data. Results for the original (radiance) data were similar except within the 700 nm to 1350 nm wavelength region. In addition, the non-derivative-band  $R^2$  values clearly outperformed the derivative-band  $R^2$  values. A stepwise multiple regression technique was applied to the entire data set (159 bands) and to a reduced set of nine bands known to be linked with physical parameters.  $R^2$  values improved to over 0.9 in both cases. The best subset extracted from the nine-band data includes bands 12(508.4 nm), 17(557.4 nm), 43(776.6 nm), 64(978.2 nm), and 138(1648.5 nm).

## 6. ACKNOWLEDGEMENT

The authors wish to thank NASA and the Inventory Branch of the British Columbia Ministry of Forests for their support of the AVIRIS data acquisition and A. Kalil for wordprocessing the manuscript.

## 7. REFERENCES

- Gong, P., R. Pu, and J.R. Miller, 1992, "Correlating Leaf Area Index of Ponderosa Pine with Hyperspectral CASI Data", Canadian Journal of Remote Sensing, Vol.18, No.4, pp.275-282.
- Rechner, A.C., and F.L. Pun, 1980, "Inflation of  $R^2$  in Best Subset Regression", Technometrics, Vol.22, pp.49-53.
- S-PLUS, 1991, "S-PLUS Reference Manual", Version 3.0, Statistical Sciences, Inc., Seattle, Washington, U.S.A.
- Staenz, K., D. Schanzer, and C. Kushigbor, 1991, "Classification of Forest Stands in British Columbia Using AVIRIS Data: A Preliminary Investigation", Proceedings of the Third Airborne Visible/Infrared Imaging Spectrometer (AVIRIS) Workshop, JPL Publication 91-28, Pasadena, California, pp.173-182.
- Teillet, P.M. and R. Santer, 1991, "Terrain Elevation and Sensor Altitude Dependence in a Semi-Analytical Atmospheric Code", Canadian Journal of Remote Sensing, Vol.17, No.1, pp.36-44.
- Wessman, L.A., J.D. Aber, and D.L. Peterson, 1989, "An Evaluation of Imaging Spectrometry for Estimating Forest Canopy Chemistry", International Journal of Remote Sensing, Vol.10, No.8, pp.1293-1316.

Table 1: Multi-band analysis of the relative reflectance data using the stepwise multiple regression technique. The band combinations were selected from (A) 159 bands (entire data set) and (B) 9 bands (12(508.4 nm), 17(557.4), 29(675.1), 43(776.6), 52(863.0), 64(978.2), 87(1199.0), 138(1648.5), and 196(2198.7)).

Bandset (# of bands)	Band Subsets (Wavelength in nm)	Coefficient of Determination ( $R^2$ )	Standard Error of Percent Crown Closure
A (1)	204(2258.3)	0.852*	13.869
(2)	84(1170.2), 93(1256.6)	0.913*	10.840
(3)	55(891.8), 58(920.6), 213(2347.8)	0.938*	9.361
(4)	52(863.0), 68(1016.6), 90(1227.8), 179(2009.7)	0.962*	7.501
(5)	52(863.0), 68(1016.6), 84(1170.2), 149(1757.3), 190(2119.1)	0.976*	6.069
B (1)	198(2198.7)	0.840*	14.408
(2)	52(863.0), 198(2198.7)	0.862*	13.670
(3)	52(863.0), 87(1199.0), 138(1648.5)	0.886*	12.708
(4)	17(557.4), 52(863.0), 87(1199.0), 138(1648.5)	0.891*	12.761
(5)	12(508.4), 17(557.4), 43(776.6), 64(978.2), 138(1648.5)	0.903*	12.294

\* passed significance test at 0.95 confidence level.

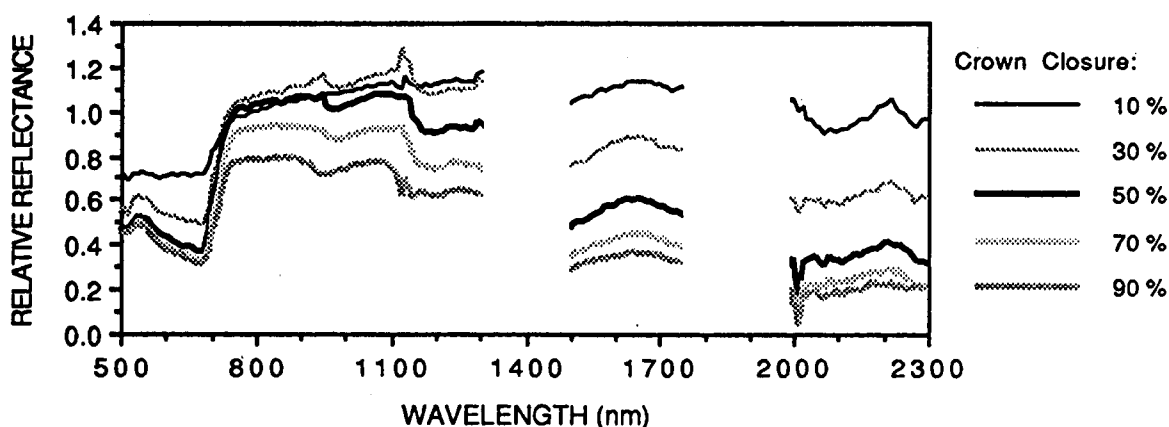


Figure 1: Relative reflectance spectra of different crown closure classes.

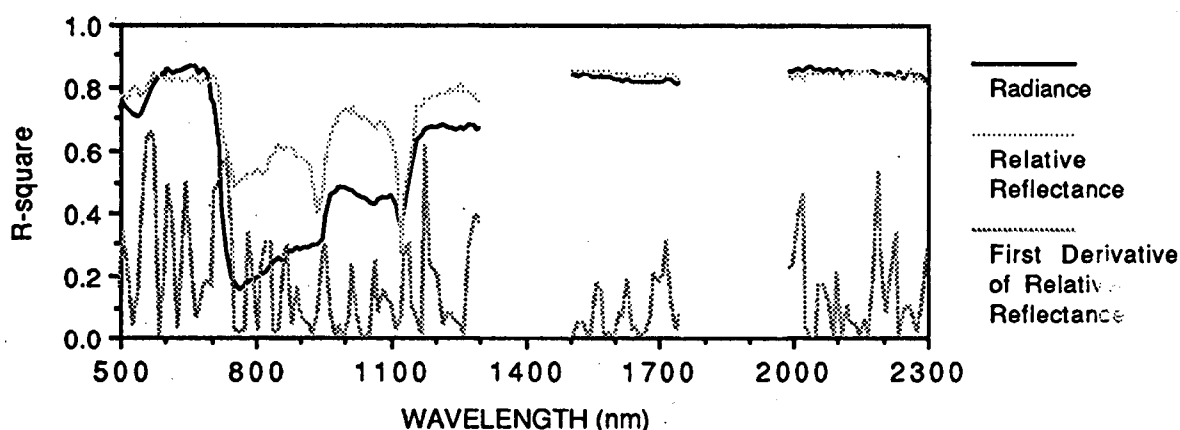


Figure 2: Correlation between percent crown closure and radiance, relative reflectance, and first-order derivative of the relative reflectance data.

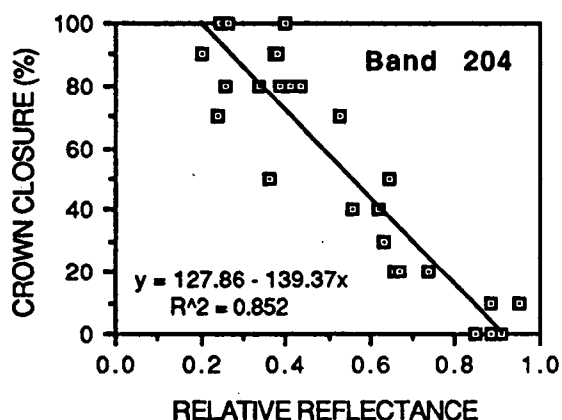


Figure 3: Crown closure as a function of the relative reflectance (atmospherically corrected data) for band 204 (2258.3 nm).

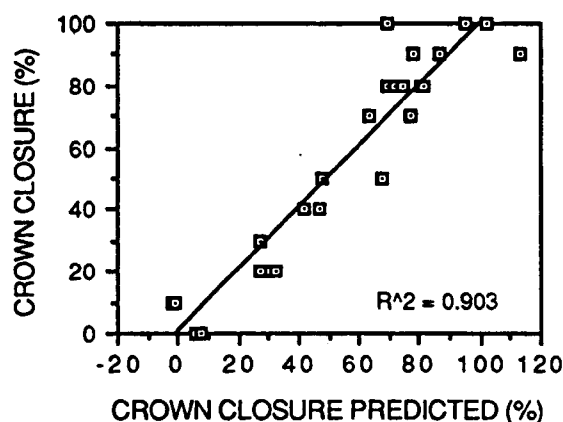


Figure 4: Prediction of crown closure derived with the stepwise multiple regression technique involving bands 12(508.4 nm), 17 (557.4 nm), 43(776.6 nm), 64(978.2 nm), and 138(1648.5 nm).